

## Backbone-Thermoresponsive Hyperbranched Polyethers

Zhifeng Jia,<sup>†,‡</sup> Hao Chen,<sup>†</sup> Xinyuan Zhu,<sup>\*,†,‡</sup> and Deyue Yan<sup>\*,†</sup>

School of Chemistry and Chemical Technology, State Key Laboratory of Metal Matrix Composites, Shanghai Jiao Tong University, 800 Dongchuan Road, Shanghai 200240, People's Republic of China, and Instrumental Analysis Center, Shanghai Jiao Tong University, 1954 Huashan Road, Shanghai 200030, People's Republic of China

Received April 5, 2006; E-mail: xyzhu@sjtu.edu.cn; dyyan@sjtu.edu.cn

Thermoresponsive dendritic polymers, which combine the advantages of dendritic polymers<sup>1,2</sup> and thermoresponsive polymers,<sup>3</sup> have attracted considerable attention. To date, two different strategies have been employed to prepare thermoresponsive dendritic polymers. One is the incorporation of temperature-responsive groups<sup>4a</sup> or polymers<sup>4b–e</sup> onto the surface of a dendrimer or hyperbranched polymer. The other is the grafting of hydrophobic and hydrophilic functionalities into a highly branched polymer,<sup>5</sup> and the temperature sensitivity is given to the dendritic polymer by the appropriate balance of hydrophilic and hydrophobic moieties. In both cases, the backbone of the dendritic polymer is not thermoresponsive, and the temperature sensitivity is imparted by modification moieties. To the best of our knowledge, the dendritic polymer with a temperature-responsive backbone has not yet been prepared. We noted that Fréchet and co-workers<sup>6</sup> had reported the synthesis of hyperbranched polymers via proton-transfer polymerization<sup>7</sup> of 1,2,7,8-diepoxyoctane and trimethylolethane (TME). The obtained hyperbranched polyethers were hydrophobic so that they were insoluble in water. It has been well realized that an appropriate combination of hydrophilic/hydrophobic balance in the polymer chains is required for the occurrence of phase transition. Therefore, it can be inferred that, if 1,2,7,8-diepoxyoctane is replaced by a more hydrophilic monomer, the hyperbranched polymer with a thermoresponsive backbone might be obtained. Fortunately, we succeeded in preparing such backbone-thermoresponsive hyperbranched polyethers by proton-transfer polymerization of 1,4-butanediol diglycidyl ether (BDE) and various triols.

The polymerization of BDE and triol was carried out in dimethyl sulfoxide (DMSO) at 40 °C through one-step polymerization. The reaction proceeded homogeneously, and no gel formation took place throughout the course of polymerization. Details of the polymerization are described in the Supporting Information. Scheme 1 gives the polymerization mechanism: The triol **1** first reacts with potassium hydride (KH) to originate the initiator **1\***. In the subsequent propagation step, the alkoxide potassium **1\*** reacts with the epoxide ring of BDE **2** and generates a secondary alkoxide **3**. Rapid proton transfer from secondary alkoxide to primary alkoxide would facilitate the formation of **4**. Finally, continuous propagation and proton transfer afford the hyperbranched polyether **5**. The experimental condition and the correspondent characterization data for the final products are listed in Table 1.

The hyperbranched architecture for the obtained polyethers was confirmed by nuclear magnetic resonance (NMR) analysis. Details of architecture elucidation and degree of branching (DB) determination can be found in the Supporting Information. The calculated DB values are summarized in Table 1. With increasing the mole ratio of BDE to TME, the DB value increases.

**Scheme 1.** Schematic Representation of Proton-Transfer Polymerization of 1,4-Butanediol Diglycidyl Ether and Triol

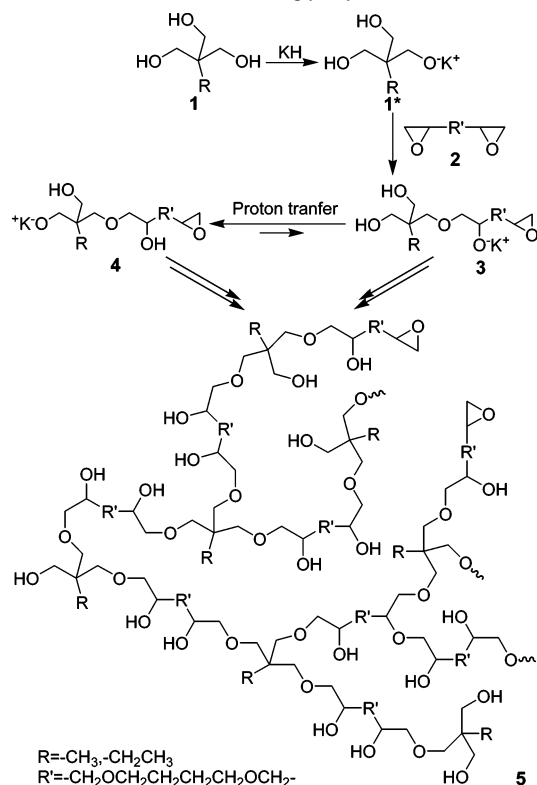


**Table 1.** Reaction Condition and Results of Proton-Transfer Polymerization of BDE and Various Triols<sup>a</sup>

No.	triol	yield (%)	$M_n^i$	$M_w/M_n^i$	DB	LCST <sup>j</sup> (°C)
1	TMP <sup>b</sup>	53	14900	3.63	0.50	19.0
2	TMP/TME <sup>c</sup>	72	10600	3.91	0.49	27.5
3	TMP/TME <sup>d</sup>	57	9300	3.23	0.47	35.7
4	TME <sup>e</sup>	68	11100	3.82	0.47	40.3
5	TME <sup>f</sup>	49	12700	3.60	0.53	36.3
6	TME <sup>g</sup>	48	12100	3.68	0.59	34.0
7	TME <sup>h</sup>	50	15900	3.19	0.63	28.1

<sup>a</sup> Reaction conditions: KH/triol = 1/4, temperature 40 °C, time 27 h. <sup>b</sup> BDE/TMP = 1/1 (mol:mol). <sup>c</sup> BDE/TMP/TME = 1/0.5/0.5. <sup>d</sup> BDE/TMP/TME = 1/0.1/0.9. <sup>e</sup> BDE/TME = 1/1. <sup>f</sup> BDE/TME = 1.2/1. <sup>g</sup> BDE/TME = 1.5/1. <sup>h</sup> BDE/TME = 2.0/1. <sup>i</sup> Molecular weights and polydispersity of the benzoyl chloride end-capped hyperbranched polymers, determined by GPC-MALLS. <sup>j</sup> Determined by UV-vis.

The hyperbranched polyethers obtained from BDE and various triols are highly soluble in water under low-temperature conditions. Interestingly, the transparent aqueous solutions of hyperbranched polyethers become opaque at a specific temperature as the temperature is increased and become transparent again when the temperature decreases. Moreover, the reversible phase transition

<sup>†</sup> School of Chemistry and Chemical Technology, State Key Laboratory of Metal Matrix Composites.

<sup>‡</sup> Instrumental Analysis Center, Shanghai Jiao Tong University.

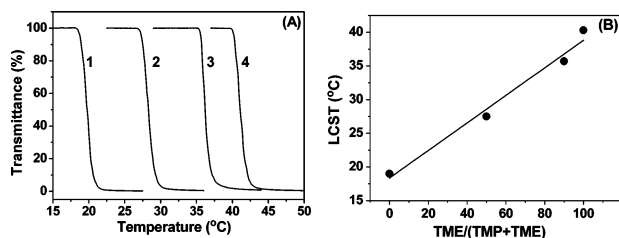


**Figure 1.** (A) Temperature dependence of light transmittance for aqueous solutions of samples 1–4. (B) Effect of TME/(TMP+TME) on LCST.

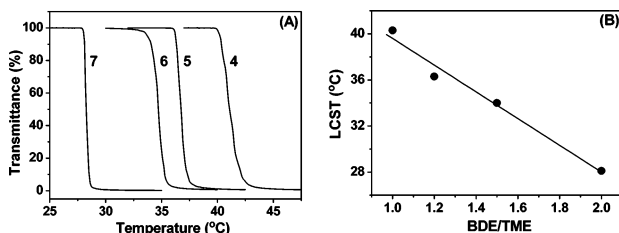


**Figure 2.** (A) Temperature dependence of light transmittance for aqueous solutions of samples 4–7. (B) Effect of mole ratio of BDE to TME on LCST.

occurs repeatedly. This phenomenon indicates that the obtained hyperbranched polyethers are temperature sensitive. The thermoresponsive behavior can be attributed to the combination of the hydrophilic groups (such as  $-\text{OH}$  and  $-\text{O}-$ ) and hydrophobic groups (such as  $-\text{CH}_3$ ,  $-\text{CH}_2\text{CH}_3$ , and  $-\text{C}_4\text{H}_9-$ ) in the polymer backbone. At the temperature above the LCST, the interaction of the hydrophobic groups drives the polymeric chains to aggregate and then separate from water.<sup>8</sup>

The phase transition temperatures were determined in water by turbidimetry measurement on a temperature-controlled UV–vis spectrometer. Figure 1A and Figure 2A demonstrate the temperature dependence of the light transmittance of 1.0 wt % aqueous solution of samples 1–7 at 500 nm. The lower critical solution temperatures (LCSTs) were defined as the temperature corresponding to 90% transmittance of aqueous solution during the heating process. As can be seen, the transmittance decreases drastically in response to a minute change of the temperature around the LCST, indicating the highly sensitive phase separation.

A series of hyperbranched polyethers were prepared from BDE and various triols, such as trimethylolpropane (TMP) and trimethylethane (TME). By increasing the hydrophilicity of triol, the LCST value of correspondent hyperbranched polyethers increases. Table 1 shows that the products prepared from TMP or TME show LCST values of 19.0 and 40.3 °C, respectively. By changing the ratio of TMP to TME, the LCST can be adjusted. Figure 1B displays the effect of the composition ratio on the phase transition behavior. It can be found that the LCST value increases almost linearly with increasing the content of TME in the range from 19.0 to 40.3 °C. Besides changing the ratio of different triols, the LCST can also be controlled by the initial mole ratio of diepoxide 2 to triol 1. Figure 2B gives the effect of mole ratio of BDE to TME on LCST. The LCST decreases linearly with increasing the mole ratio of BDE to TME. These data suggest that LCST values can be easily adjusted at any desired temperature between 19.0 and 40.3 °C by controlling the hydrophilic–hydrophobic balance of BDE and various triols.

In conclusion, a new type of materials, the backbone-thermo-responsive hyperbranched polyether, has been successfully synthe-

sized by proton-transfer polymerization of 1,4-butanediol diglycidyl ether (BDE) and various triols. Importantly, the LCST values can be readily adjusted from 19.0 to 40.3 °C by changing either the ratio of different triols or the ratio of BDE to TME. The hyperbranched polyether with a thermoresponsive backbone has a large number of hydroxyl and epoxide groups at the chain ends; therefore it is a potential intelligent matrix for further modification. For example, functional molecules, such as drug and probe, can be easily introduced, allowing favorable applications. Further studies on the backbone-thermo-responsive hyperbranched polymers and their functionalization are underway in our laboratory.

**Acknowledgment.** The authors gratefully acknowledge the financial support from the National Natural Science Foundation of China (20574044 and 50233030) and the Basic Research Foundation of Shanghai Science and Technique Committee (Nos. 03JC14046, 04JC14057, and 05DJ14005).

**Supporting Information Available:** Full experimental details and characterization data. This material is available free of charge via the Internet at <http://pubs.acs.org>.

## References

- (1) (a) Fréchet, J. M. J.; Tomalia, D. A. In *Dendrimers and Other Dendritic Polymers*; John Wiley & Sons: New York, 2001. (b) Bosman, A. W.; Janssen, H. M.; Meijer, E. W. *Chem. Rev.* **1999**, *99*, 1665. (c) Fréchet, J. M. J. *Science* **1994**, *263*, 1710. (d) Stiriba, S. E.; Frey, H.; Haag, R. *Angew. Chem., Int. Ed.* **2002**, *41*, 1329. (e) Vögtle, F.; Gestermann, S.; Hesse, R.; Schwier, H.; Windisch, B. *Prog. Polym. Sci.* **2000**, *25*, 987.
- (2) (a) Kim, Y. H.; Webster, O. W. *J. Am. Chem. Soc.* **1990**, *112*, 4592. (b) Coessens, V.; Pintauer, T.; Matyjaszewski, K. *Prog. Polym. Sci.* **2001**, *26*, 337. (c) Jikei, M.; Kakimoto, M. *Prog. Polym. Sci.* **2001**, *26*, 1233. (d) Hawker, C. J.; Lee, R.; Fréchet, J. M. J. *J. Am. Chem. Soc.* **1991**, *113*, 4583. (e) Markoski, L. J.; Thompson, J. L.; Moore, J. S. *Macromolecules* **2002**, *35*, 1599. (f) Simon, P. F. W.; Müller, A. H. E.; Pakula, T. *Macromolecules* **2001**, *34*, 1677. (g) Höltzer, D.; Frey, H. *Acta Polym.* **1997**, *48*, 298. (h) Voit, B. *J. Polym. Sci., Polym. Chem. Ed.* **2000**, *38*, 2505. (i) Hult, A.; Johansson, M.; Malmström, E. *Adv. Polym. Sci.* **1999**, *143*, 1.
- (3) (a) McCormick, C. L. In *Stimuli-Responsive Water Soluble and Amphiphilic Polymers*; ACS Symposium Series 780; American Chemical Society: Washington, DC, 2001. (b) Gil, E. S.; Hudson, S. M. *Prog. Polym. Sci.* **2004**, *29*, 1173. (c) Kost, J.; Langer, R. *Adv. Drug Delivery Rev.* **2001**, *46*, 125. (d) Jeong, B.; Kim, S. W.; Bae, Y. H. *Adv. Drug Delivery Rev.* **2002**, *54*, 37. (e) Galaev, I. Y.; Mattiasson, B. *Trends Biotechnol.* **1999**, *17*, 335. (f) Tanaka, T. *Phys. Rev. Lett.* **1978**, *40*, 820. (g) Hoffman, A. S. *J. Controlled Release* **1987**, *6*, 297. (h) Osada, Y.; Gong, J. P. *Adv. Mater.* **1998**, *10*, 827.
- (4) (a) Haba, Y.; Harada, A.; Takagishi, T.; Kono, K. *J. Am. Chem. Soc.* **2004**, *126*, 12760. (b) You, Y. Z.; Hong, C. Y.; Pan, C. Y.; Wang, P. H. *Adv. Mater.* **2004**, *16*, 1953. (c) Kimura, M.; Kato, M.; Muto, T.; Hanabusa, K.; Shirai, H. *Macromolecules* **2000**, *33*, 1117. (d) Kojima, C.; Haba, Y.; Fukui, T.; Kono, K.; Takagishi, T. *Macromolecules* **2003**, *36*, 2183.
- (5) (a) Aathimanikandan, S. V.; Savariar, E. N.; Thayumanavan, S. *J. Am. Chem. Soc.* **2005**, *127*, 14922. (b) Parrott, M. C.; Marchington, E. B.; Valliant, J. F.; Adronov, A. *J. Am. Chem. Soc.* **2005**, *127*, 12081. (c) Gillies, E. R.; Jonsson, T. B.; Fréchet, J. M. J. *J. Am. Chem. Soc.* **2004**, *126*, 11936. (d) Gitsov, I.; Fréchet, J. M. J. *J. Am. Chem. Soc.* **1996**, *118*, 3785.
- (6) (a) Emrick, T.; Chang, H. T.; Fréchet, J. M. J. *Macromolecules* **1999**, *32*, 6380. (b) Emrick, T.; Chang, H. T.; Fréchet, J. M. J. *J. Polym. Sci., Polym. Chem. Ed.* **2000**, *38*, 4850.
- (7) (a) Chang, H. T.; Fréchet, J. M. J. *J. Am. Chem. Soc.* **1999**, *121*, 2313. (b) Gong, C. G.; Fréchet, J. M. J. *Macromolecules* **2000**, *33*, 4997. (c) Hecht, S.; Emrick, T.; Fréchet, J. M. J. *Chem. Commun.* **2000**, 313. (d) Sunder, A.; Hanselmann, R.; Frey, H.; Mülhaupt, R. *Macromolecules* **1999**, *32*, 4240. (e) Imai, T.; Satoh, T.; Kaga, H.; Kaneko, N.; Kakuchi, T. *Macromolecules* **2003**, *36*, 6359. (f) Imai, T.; Nawa, Y.; Kitaiyo, Y.; Satoh, T.; Kaga, H.; Kaneko, N.; Kakuchi, T. *Macromolecules* **2005**, *38*, 1648–1654.
- (8) (a) Chen, G.; Hoffman, A. S. *Nature* **1995**, *373*, 49. (b) Heskins, M.; Guillet, J. E. *J. Macromol. Chem. A2* **1968**, 1441.

JA062314D

## Supporting Information

### Backbone-thermoreponsive hyperbranched polyethers

Zhifeng Jia<sup>1,2</sup>, Hao Chen<sup>1</sup>, Xinyuan Zhu<sup>1,2\*</sup>, and Deyue Yan<sup>1\*</sup>

<sup>1</sup> *School of Chemistry and Chemical Technology, State Key Laboratory of Metal Matrix Composites, Shanghai Jiao Tong University, 800 Dongchuan Road, Shanghai 200240, People's Republic of China*

<sup>2</sup> *Instrumental Analysis Center, Shanghai Jiao Tong University, 1954 Huashan Road, Shanghai 200030, People's Republic of China*

<b>S1 Experimental details</b>	<b>S-1</b>
<b>S2 Photograph of the behavior of phase transition</b>	<b>S-2</b>
<b>S3 Characterization of hyperbranched polyethers</b>	<b>S-3</b>
<b>S4 Determination of the degree of branching</b>	<b>S-4</b>

#### S1 Experimental details

##### S1.1 Materials.

Trimethylolpropane (TMP, Acros), trimethylolethane (TME, Acros) glycerol (Aldrich), 1,4-butanediol diglycidyl ether (BDE, Aldrich), potassium hydride (KH, 30 wt% dispersion in mineral oil, Aldrich) used as received. Tetrahydrofuran (THF) was purified by refluxing over fresh sodium-benzophenone complex (a deep purple color indicating an oxygen- and moisture-free solvent) and distilled before polymerization. Dimethyl sulfoxide (DMSO) was dried over calcium hydride (CaH<sub>2</sub>) and distilled under reduced pressure.

##### S1.2 Polymerization.

A typical polymerization procedure is as follows (Table 1, entry 1): A suspension of KH in mineral oil (30 % in weight) was introduced in a dry pre-weighted 50 mL

Schlenk flask under argon. The mineral oil was removed by three extractions with THF added to the flask by syringe. The remaining THF was removed by vacuum. When KH was completely dried, the flask was weighted to determine the amount of KH (0.101 g, 2.52 mmol). Then 20 mL DMSO and TMP (1.348 g, 10.05 mmol) was introduced into the flask. The solution was maintained for 30 min to form the alcoholate potassium. BDE (2.041 g, 10.09 mmol) was added by syringe and the polymerization was conducted for 27 h at 40 °C and then precipitated into acetone/diethyl ether (v/v=1/4). The product was dissolved in methanol and neutralized by filtration over cation-exchange resin. The polymer was precipitated twice from methanol solution into cold diethyl ether and subsequently dried under vacuum. The polymeric product was obtained as a highly viscous liquid.

### **S1.3 End-capping reaction.**

To the mixture of the polymer (0.2 g), triethylamine (1 mL) and dried THF (10 mL), benzoyl chloride (1.5 mL) in 2 mL THF was added at 0 °C. The reaction mixture was stirred at room temperature for 24 h under argon atmosphere. The end-capped products were purified with column chromatography on silica gel and CH<sub>2</sub>Cl<sub>2</sub> was used as the elution solvent.

### **S1.4 Measurements.**

**Nuclear Magnetic Resonance (NMR).** The one-dimensional and two-dimensional NMR spectra were recorded using Varian MERCURY plus-400 spectrometer with dimethyl sulfoxide-*d*<sub>6</sub> (DMSO-*d*<sub>6</sub>) as solvent. Quantitative <sup>13</sup>C NMR spectra were measured by the method of inverse gated <sup>1</sup>H decoupling. In DEPT experiments, the <sup>1</sup>H tip angle  $\theta$  was set to 135° to determine carbon multiplicities with CH, CH<sub>3</sub> up and CH<sub>2</sub> down. <sup>1</sup>H, <sup>1</sup>H-COSY and <sup>13</sup>C, <sup>1</sup>H-HSQC spectra were recorded using the standard pulse sequence provided by Varian.

**Gel Permeation Chromatography (GPC).** The molecular weight and molecular weight distribution were determined by gel permeation chromatography/multi-angle laser light scattering (GPC-MALLS). The gel permeation chromatography system consists of a Waters degasser, a Waters 515 HPLC pump, a 717 automatic sample injector, a Wyatt Optilab DSP differential refractometer detector, and a Wyatt

miniDAWN multi-angle laser light scattering detector. Three chromatographic columns (styragel HR3, HR4, and HR5) were used in series. THF was used as the mobile phase at a flow rate of 1 mL/min at 30 °C. The refractive index increment  $dn/dc$  was determined with Wyatt Optilab DSP differential refractometer at 690 nm. Data analysis was performed with Astra software (Wyatt Technology).

**Differential Scanning Calorimetry (DSC).** The glass transition temperatures ( $T_g$ ) of obtained hyperbranched polymers were determined using a Perkin-Elmer Pyris 1 differential scanning calorimeter in a dry nitrogen atmosphere. All samples were heated to 100 °C from -100 °C at a rate of 10 °C/min. The midpoint of the slope change of the heat capacity plot of the second heating scan was taken as  $T_g$ .

**Lower Critical Solution Temperature (LCST) Measurement.** The LCST of the polymer solutions (1 wt%) were measured by monitoring the transmittance of a 500 nm light beam using a GBC Cintra 10e UV-visible spectrometer equipped with a thermal cell. The temperature of the solution was increased at a rate of 0.5 °C/min.

## S2 Photograph of the behavior of phase transition



**Figure S-1.** The photographs of 1.0 wt% aqueous solution of sample 4 at 30 °C (left) and 50 °C (right).

## S3 Characterization of hyperbranched polyethers

The molecular weight and molecular weight distribution of the obtained hyperbranched polyethers were determined by GPC-MALLS. To avoid interaction of the polymer with the column packing, the hydroxyl groups were end-capped with benzoyl chloride before GPC-MALLS characterization. The molecular weights of

hyperbranched polyethers are given in Table 1. It should be mentioned that benzylation of the hydroxyl end groups increases the molecular weight of the sample.

Hyperbranched polyether **5** shows good solubility in polar solvents, such as DMSO, DMF and methanol, but it is insoluble in chloroform. The end-capping polymer with benzoyl chloride is soluble in THF, chloroform, but insoluble in methanol.

Differential scan calorimetry (DSC) measurements show that the glass transition temperatures ( $T_g$ ) of the obtained polyethers range from -26.7 to -35.2 °C.

#### S4 Determination of the degree of branching

The structure of the resulting polymers was analyzed by  $^1\text{H}$  NMR and  $^{13}\text{C}$  NMR spectroscopy. In the  $^1\text{H}$  NMR spectrum of sample 1 (Figure S-2a), the methyl and methylene protons from TMP units appear at 0.76 and 1.22 ppm, respectively. In the  $^1\text{H}$  NMR spectrum of sample 6 (Figure S-2b), the methyl protons from TME units appeared at 0.70-0.85 ppm. The appearance of the characteristic peaks from TMP or TME units confirms the incorporation of TMP or TME into the polymer structure. The signals at 1.50 ppm are the characteristic absorption of methylene protons ( $-\text{OCH}_2\text{CH}_2\text{CH}_2\text{CH}_2\text{O}-$ ). The broad signals at 3.15-3.70 ppm are assigned to the methylene and methine protons adjacent to oxygen of ether and alcohol moieties. The characteristic absorptions at 2.54-3.10 ppm due to the epoxy protons are observed. Hydroxyl protons give signals at 4.24-4.78 ppm.

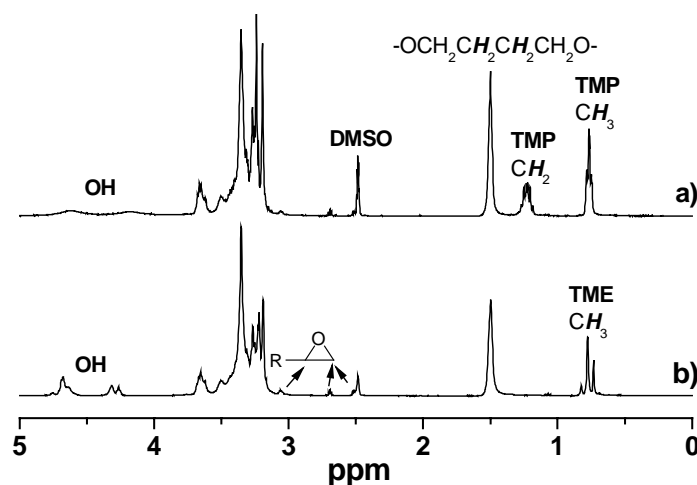


**Figure S-2.**  $^1\text{H}$  NMR spectra of samples 1 (a) and 6 (b).

As can be seen from Figure S-2b, the methyl protons are divided into three

resonances at 0.82, 0.78, 0.73 ppm, which correspond to trisubstituted, disubstituted and monosubstituted units of the TME unit respectively. The percentage of trisubstituted and disubstituted units increases with increasing the ratio of BDE to TME (see Table S-1). Compared with the percentage of disubstituted and monosubstituted units, the percentage of trisubstituted unit is rather lower. This may be due to the higher steric hindrance of trisubstitution reaction. As expected, the percentage of epoxide group also increases with increasing the ratio of BDE to TME.

**Table S-1.** The percentage of trisubstituted, disubstituted and monosubstituted units.

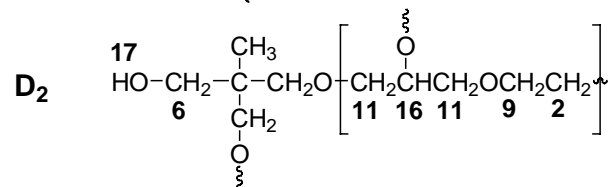
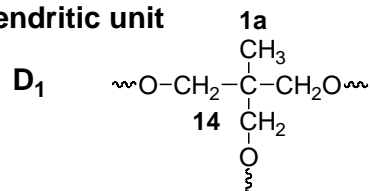
Entry	BDE/triol	Trisubstitute (%)	Disubstitute (%)	Monosubstitute (%)	Epoxide (%)
4	1.0	7.1	56.3	36.6	3.3
5	1.2	8.3	58.9	32.8	11.8
6	1.5	10.4	62.6	27.0	15.9
7	2.0	12.6	66.0	21.4	25.7

Careful examination of the structure of polymer **5** reveals that seven different types of subunits D<sub>1</sub>, D<sub>2</sub>, T<sub>1</sub>, T<sub>2</sub>, L<sub>1</sub>, L<sub>2</sub> and L<sub>3</sub> may be present. Chart S-1 displays the structural units of hyperbranched polyether synthesized from BDE and TME.

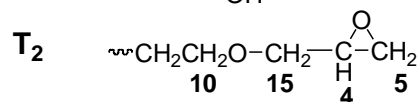
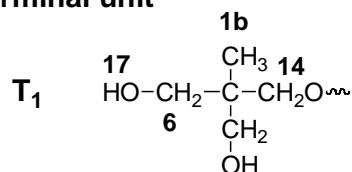
Figure S-3 shows the quantitative <sup>13</sup>C NMR and <sup>13</sup>C DEPT-135 NMR spectra of sample 5. DEPT-135 spectra can be employed to distinguish methylene and methane or methine carbons (Figure S-3a). According to the DEPT spectrum, the peak **1** is assigned to the methyl groups from TME units. The epoxide resonances are observed at peaks **4** and **5**. The peaks **7**, **8** and **16** are attributed to R<sub>2</sub>CH-OH and R<sub>2</sub>CH-OR, respectively. The peak **3** is assigned to quaternary carbon atom, which shows no signal in the corresponding DEPT spectra.

**Chart S-1.** Structure units of the hyperbranched polyethers **5**.

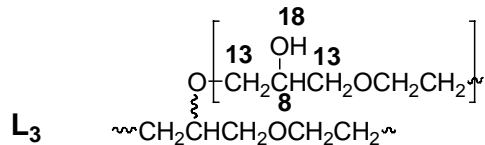
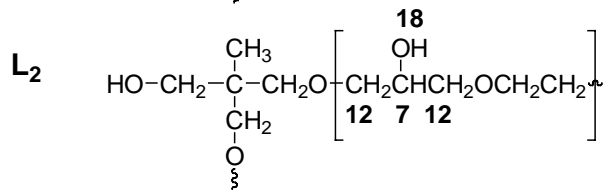
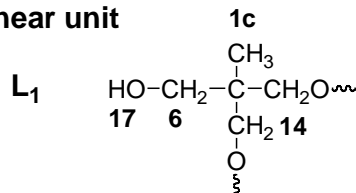
### Dendritic unit



### Terminal unit



### Linear unit



The  $^1\text{H}$ ,  $^1\text{H}$ -COSY (Figure S-4) and  $^{13}\text{C}$ ,  $^1\text{H}$ -HSQC spectra (Figure S-5) were performed for further assignment of the peaks. Chart S-1 reveals that 2-H/9-H, 4-H/15-H, 5-H/5-H, 6-H/17-H, 7-H/12-H, 8-H/13-H, 7-H/18-H, 8-H/18-H are in different spin system. The cross peaks in Figure S-4 and S-5 would facilitate assignment of these systems. Using the information obtained from the  $^1\text{H}$ ,  $^1\text{H}$ -COSY and  $^{13}\text{C}$ ,  $^1\text{H}$ -HSQC spectra, the detailed assignment is shown in Figure S-3b.



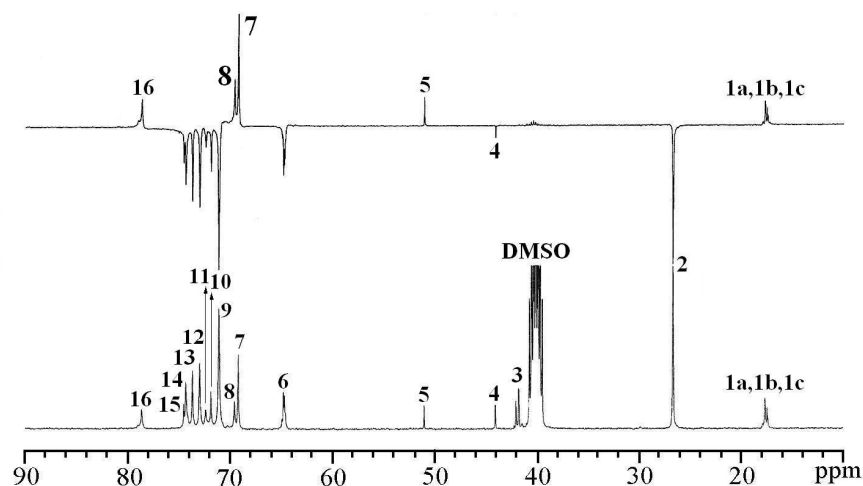


**Figure S-3.** DEPT-135 (a) and quantitative  $^{13}\text{C}$  NMR (b) spectra of sample 5.

The DB can be calculated on the basis of the intensity of NMR from the fraction of structural units using the following equation:

$$\text{DB} = (\text{D}+\text{T})/(\text{D}+\text{T}+\text{L}) = (\text{D}_1+\text{D}_2+\text{T}_1+\text{T}_2)/(\text{D}_1+\text{D}_2+\text{T}_1+\text{T}_2+\text{L}_1+\text{L}_2+\text{L}_3)$$

Where  $\text{D}_1$ ,  $\text{D}_2$ ,  $\text{T}_1$ ,  $\text{T}_2$ ,  $\text{L}_1$ ,  $\text{L}_2$  and  $\text{L}_3$  represent the fractions of the dendritic  $\text{D}_1$ ,  $\text{D}_2$ , terminal  $\text{T}_1$ ,  $\text{T}_2$ , and linear  $\text{L}_1$ ,  $\text{L}_2$ ,  $\text{L}_3$  units, respectively. Table 1 shows that the DB values for hyperbranched polyethers range from 0.47 to 0.63.

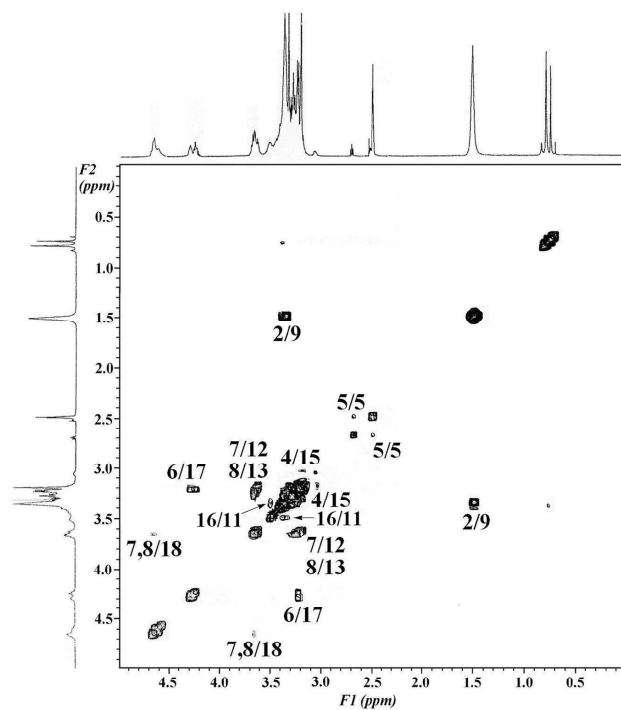


**Figure S-4.**  $^1\text{H}$ ,  $^1\text{H}$ -COSY spectrum of sample 5

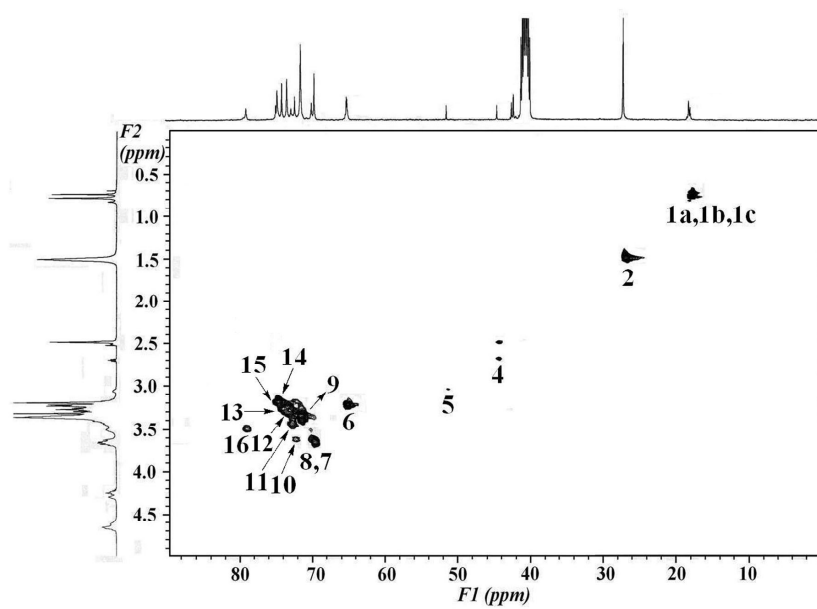


**Figure S-5.**  $^{13}\text{C}$ ,  $^1\text{H}$ -HSQC spectrum of sample 5